BODIPY fluorescent dyes for selective staining of intracellular organelles

Mladena Glavaš,[a‡] Lorena Vidoša,[a,b‡] Martina Mušković,[b‡] Ivana Ratkaj,[b*] and Nikola Basarić[a*]

[a] Department of Organic Chemistry and Biochemistry, Ruđer Bošković Institute, Bijenička cesta 54, 10 000 Zagreb, Croatia E-mail: nbasaric@irb.hr

[b] Faculty of Biotechnology and Drug Development, University of Rijeka, Radmile Matejčić 2, 51 000 Rijeka, Croatia E-mail: IR iratkaj@biotech.uniri.hr

[‡] The authors marked with ‡ contributed equally and can be considered as the first (main) authors.

TOC:

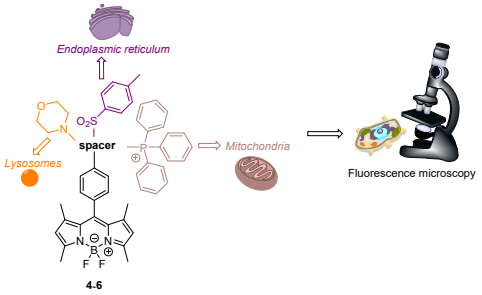

Abstract: By use of a simple synthetic methodology for peptide coupling by HATU reagent, two BODIPY amides **4** and **5** were synthesized, that were at the *meso*-position substituted with a morphline moiety targeting lysosomes, or sulfonamide group targeting endoplasmic reticulum (ER), respectively. Furthermore, by use of Cu-catalyzed click chemistry, dye **6** was synthesized from a BODIPY alkyne, that was at the *meso*-position substituted with a triphenylphosponium salt via a triazol linker, for targeting mitochondria. Photophysical and spectral properties of BODIPY dyes **4-6** were characterized in nonpolar, polar aprotic and protic solvent. All compounds in all solvents have high values of fluorescence quantum yields (Φ_F = 0.5-0.8), and single-exponential decay of fluorescence with singlet excited state lifetimes τ = 2.5-3.8 ns. The substituents in the *meso*-position that direct the dyes towards different intracellular organelles do not affect the photophysical properties. Moreover, the stability of amides **4** and **5** was tested with lipases CAL-B and PPL, whereupon they showed hydrolytic stability. The applicability of dyes **4-6** in fluorescent staining of organelles in HeLa cell line was tested in colocalization microscopy studies with commercial dyes Lysotracker RED, ER tracer and Mitotracker Red. They showed excellent localization in lysosomes, ER and mitochondria with the values of Pearson's coefficients 0.90, 0.94, and 0.93, respectively. Consequently, BODIPY derivatives **4-6** have potential to be used in biology as selective organelle targeting dyes. Moreover, our simple synthetic protocol for the preparation of dyes in principle allows for the synthesis of plethora of different BODIPY derivatives with selective localization in different organelles.

Key words: BODIPY, fluorescence microscopy, endoplasmic reticulum, lysosomes, mitochondria, photophysical properties

Introduction

Fluorescence microscopy is a powerful technique often used in biology, which allows for observation of various processes in living cells and organisms.[1] It relies on the use of fluorescent dyes, which are expected to show specific fluorescent response depending on their localization and environment.[2] Although a large number of commercially available fluorescent dyes for biology and microscopy are on the market,[3] neither one is universally perfect for different applications, characterized by desirable spectral and photophysical properties and selective response in bio-environment. Consequently, there is a constant demand for new and better fluorescent dyes for different applications, such as selective localization in intracellular organelles.[4]

BODIPY dyes are a popular class of heterocyclic compounds, that are derivatives of 4,4-difluoro-4-bora-3a,4a-diaza-*s*-indacene, first time synthesized by Triebs and Kreuzer.[5] These fluorescent dyes are mostly characterized by exceptional spectroscopic and photophysical properties,[6,7] which can be easily tuned by simple structural modifications.[8,9] Therefore, these dyes found widespread use in material science,[10] fluorescence sensing,[11] and anti-cancer phototherapeutics.[12] Moreover, researchers devoted a particular endeavor to develop applications in molecular biology and medicine where they have been used as fluorescent markers,[13] or photo-cleavable protective groups (also known as photocages)[14,15] with applications in medicine,[16,17] and super resolution microscopy in biology.[18,19,20,21] BODIPY dyes have been structurally modified to specifically localize in membranes,[21] mitochondria,[13,19,22] lysosomes,[23] endoplasmic reticulum (ER),[24] Golgy apparatus,[25] or cell nucleus,[26] and some representative examples are shown in Fig 1.

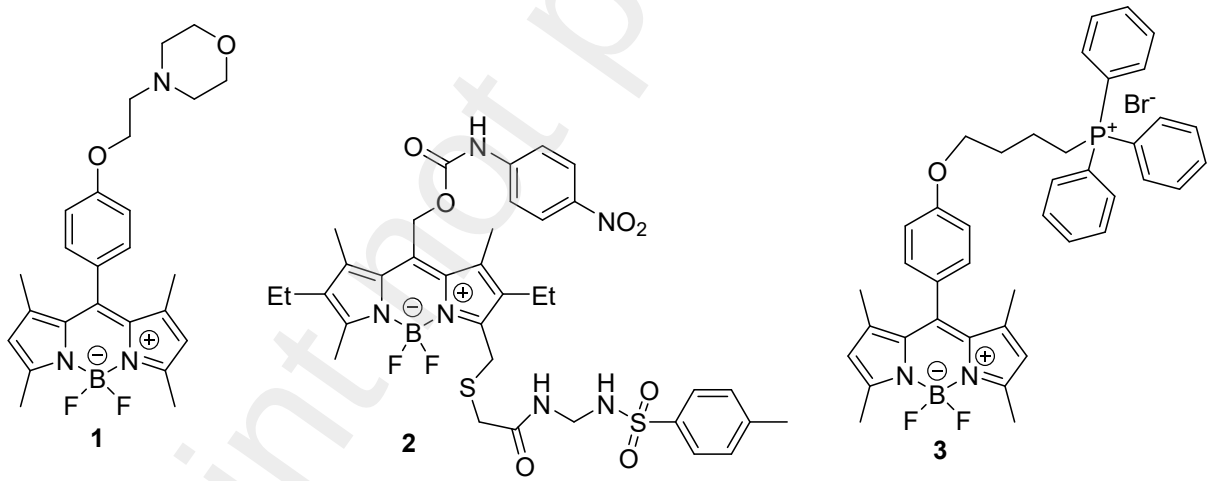

Fig 1. Fluorescent dyes for selective staining of lysosomes,[23d,27] endoplasmic reticulum[19] and mitochondria[28] from literature precedent.

The intracellular localization of drugs is very important for determining their activity and mechanism of action. It is very beneficiary to design new drugs that target important cellular organelles. In cancer, for example, mitochondria play a crucial role in the regulation of apoptosis and "aerobic glycolysis",[29] the ER in the folding of secretory and membrane proteins and in calcium homeostasis,[30] while dysfunction of lysosomes can lead to an accumulation of undegraded substrates.[31] Targeting those organelles could lead to therapeutic effect of the new drugs and their possible overcoming of the most critical limitation of drug action, multidrug resistance.[32] Therefore, the development of localizing agents from the rational synthesis that

selectively target organelles of interest for biomedical applications is of critical interest for new drugs. Although different dyes for targeting organelles are available, their general drawback is often the lack of selectivity, or complicated structure and/or demanding synthesis and high cost.

Herein we present two simple synthetic methodologies which can be used to modify commercially or easily available BODIPY structures into specific organelle selective fluorescent dyes. The protocols are based on simple amide formation by use of peptide-activating reagents such as HATU, or the Cu-catalyzed click reaction. By using these protocols, we prepared fluorescent dyes **4**-**6** (for the structures see later, Schemes 1 and 2) characterized their spectral and photophysical properties and showed their applicability in selective staining of lysosomes, endoplasmic reticulum, and mitochondria. The structure of the BODIPY dyes was designed based on the known BODIPY organelle targeting reagents (Fig 1). The simple synthetic methodology in principle allows for applying these procedures for different targets, enabling rational design and construction of a plethora of fluorescent dyes for bio-medicinal applications.

Results and Discussion

Synthesis

Fluorescent dyes for staining of lysosomes, **4**, and ER, **5**, were prepared in excellent yields, from BODIPY carboxylic acid **7** (Scheme 1) by use of HATU peptide coupling reagent.[33] Thus, the use of starting compound **7** allows for the synthesis of different organelle targeting dyes in a very simple synthetic methodology. The synthetic procedure for the preparation of **7** is given in the SI.

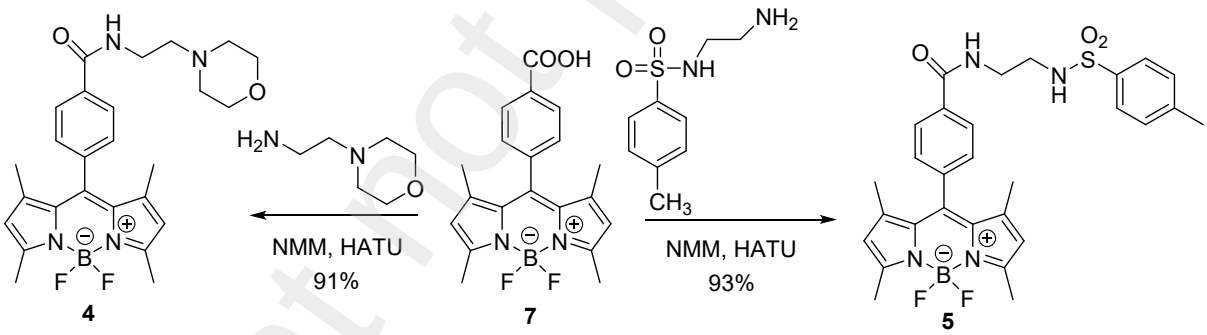

Scheme 1. Synthesis of BODIPY compounds **4** and **5** by the HATU peptide coupling protocol (NMM = *N*-methylmorpholine).

The synthetic protocol for the preparation of mitochondria targeting dye **6** is based on the preparation of BODIPY alkyne **8** and its click reaction[34] with the azide containing triphnylphosphonium salt **10** (Scheme 2). The procedures for the synthesis of precursors **9** and **10** is provided in the SI. This synthetic protocol also in principle enables preparation of different organelle targeting dyes by clicking **8** to different azides.

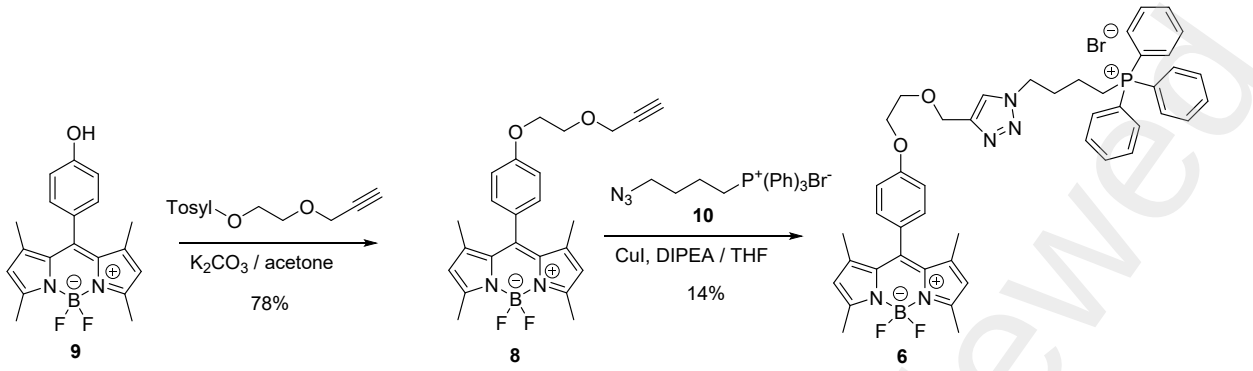

Scheme 2. Synthesis of BODIPY compound **6**.

For the application of fluorescent dyes, it is important to test their stability, particularly for the amides such as **4** and **5**, which can undergo enzymatic cleavage in cells. The stability towards lipase activity was determined using lipase B candida antartica (CAL-B)[35] and triacylglycerol lipase (PPL),[36] which are ubiquitous lipases with high catalytic efficiency, often used as catalysts. Due to unavailability of an analogous human lipase, we assumed that CAL-B and PPL would be appropriate models for checking the stability, owing to a large scope of different substrates that can be hydrolyzed, including amides, and high catalytic efficiency and stability.[35,36] Amides **4** and **5** were treated with enzymes, and HPLC analysis after 24 h revealed no hydrolysis (for details see the SI Figs S1-S10), confirming their stability under enzymatic conditions and applicability for intracellular imaging.

Photophysical Properties

Spectral and photophysical properties of **4**-**6** were investigated in nonpolar solvent CH_2Cl_2, polar aprotic CH_3CN, and in the polar protic solvent CH_3CN-H_2O (1:10 v/v) to probe for plausible photoinduced electron transfer (PET) of charge transfer (CT) processes of the dyes.[11,37] Namely, substitution of the BODIPY by alkyl groups containing tertiary amines,[38] or tertiary anilines[39] is known to enable PET from the amine to the dye and quench fluorescence, which should be affected by the change of solvent polarity and protonation of the amine by H_2O. Furthermore, BODIPY in the excited state can be an electron donor if the molecule is substituted by electron withdrawing groups, also leading to the PET and fluorescence quenching.[40]

BODIPY dyes **4**-**6** are characterized by absorption spectra with a maximum at ≈ 497-498 nm, and molar absorption coefficients 35000-100000, corresponding to the $S_0 \rightarrow S_1$ transition, the typical of BODIPY.[6,7] At 300-400 nm, weaker and broader absorption band corresponds to the excitation to higher excited states. The absorption spectra show negligible solvatochromic shifts (4 nm), and the organelle directing group in the *meso*-position does not affect the absorption properties, except absorptivity (Fig. 1 left).

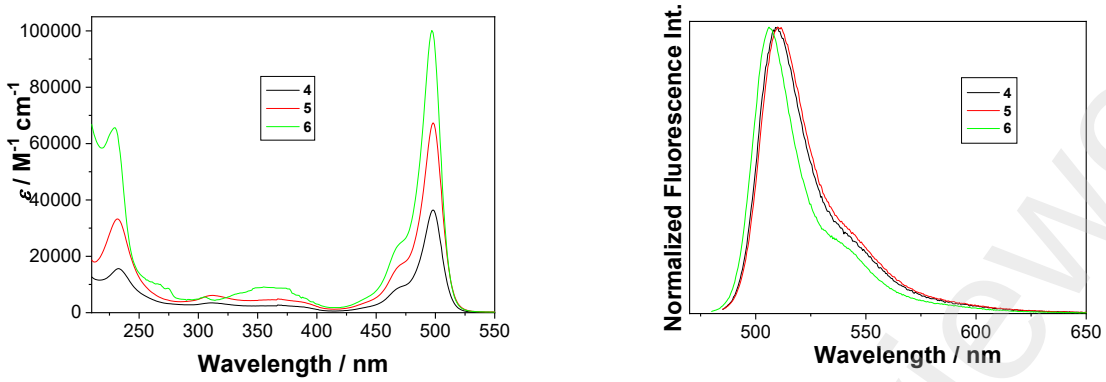

Fig 1. Absorption spectra of **4-6** in CH_3CN (left) and normalized fluorescence spectra (λ_{ex} = 470 nm) of **4-6** in CH_3CN (right).

The fluorescence spectra of **4-6** are the mirror-image of the absorption $S_0 \rightarrow S_1$ band with maxima in the CH_3CN solution at 506-510 nm (Fig. 1, right). The fluorescence spectra also show very weak solvatochromic shifts (Figs S11-S13 in the SI). The most bathochromically shifted maximum was observed in CH_2Cl_2 (514 nm), whereas the maxima in CH_3CN and in aqueous CH_3CN almost coincide (at 506 nm for **6** and 510 nm for **4** and **5**). Thus, the observed solvatochromic shifts are more reflection of the solvent polarizability then polarity, which has been reported for many BODIPY derivatives.[41]

Fluorescence quantum yields (Φ_F) for **4-6** in different solvents were determined by use of rhodamine B in CH_3OH as a reference (Φ_F = 0.66),[42] whereas the lifetimes of singlet excited states were determined by time-correlated single photon counting (TC-SPC) method (Table 1). The Φ_F values of **4-6** are similar, somewhat higher in nonpolar then in polar solvent, and the proticity of the solvent did not much affect these values. The finding indicates that the organelle targeting group in the *meso*-position did not affect the photophysical properties. In compounds **4-6**, regardless on the group in the *meso*-position, deactivation from the singlet excited state does not involve PET or pronounced CT character of the S_1 states. The decays of the fluorescence were for all compounds and in all solvents fit to single exponential function, revealing singlet excited state lifetimes in the range 2.5-3.8 ns, the typical for BODIPY derivatives.[6,7] Most importantly, relatively high values of Φ_F for **4-6** in aqueous solvent and their single-exponential fluorescence decay render these molecules as excellent dyes for fluorescence microscopy and intracellular measurements.

Table 1. Photophysical properties of BODIPY dyes **4-6** in different solvents.

Comp.	Solvent	Φ_F [a]	τ/ns [b]
4	CH_2Cl_2	0.70 ± 0.02	2.73 ± 0.02
	CH_3CN	0.55 ± 0.01	2.60 ± 0.02
	CH_3CN-H_2O (1:10)	0.51 ± 0.05	3.00 ± 0.01
5	CH_2Cl_2	0.75 ± 0.02	2.59 ± 0.02
	CH_3CN	0.50 ± 0.01	2.57 ± 0.02
	CH_3CN-H_2O (1:10)	0.51 ± 0.02	2.70 ± 0.01
6	CH_2Cl_2	0.78 ± 0.02	3.45 ± 0.01
	CH_3CN	0.54 ± 0.06	3.37 ± 0.01

	CH_3CN-H_2O (1:10)	0.62 ± 0.03	3.83 ± 0.01

[a] Quantum yiled of fluorescence measured by use of rhodamine B in CH_3OH as a reference (Φ_F = 0.66).[42] [b] Lifetimes of the singlet excited state measured by TC-SPC.

Fluorescence Microscopy

Fluorescence microscopy was used to determine whether the synthesized BODIPY dyes are localizing in the organelles of interest. BODIPY **4** (green) was tested at a concentration of 1 μM with the incubation time of 1h in serum-free medium and using Lysotracker RED as the colocalizing agent. Results indicate that **4** has a strong localization in the lysosomes, which is evident by yellow coloring of the merged images (Fig. 2). In addition, the Pearson correlation coefficient was calculated and its value of 0.90 confirms the observed localization. The localization of BODIPY **5** in the endoplasmic reticulum (ER) was tested after only 30 min of incubation and in DMEM with the ER tracer. The yellow color in the merged image of Fig. 3. and the calculated Pearson's correlation coefficient of 0.94 strongly confirms that **5** is localized in the ER within 30 minutes of incubation. For cellular localization of BODIPY **6** (green) we used Mitotracker RED, since this compound was synthesized with triphenylphosphonium group, known to target mitochondria. An overlap of the green fluorescence of the compound and the RED fluorescence of the tracker results in a yellow color of the merged image in Fig. 4. This confirms the localization of **6** in mitochondria together with the calculated Pearson's coefficient of 0.93.

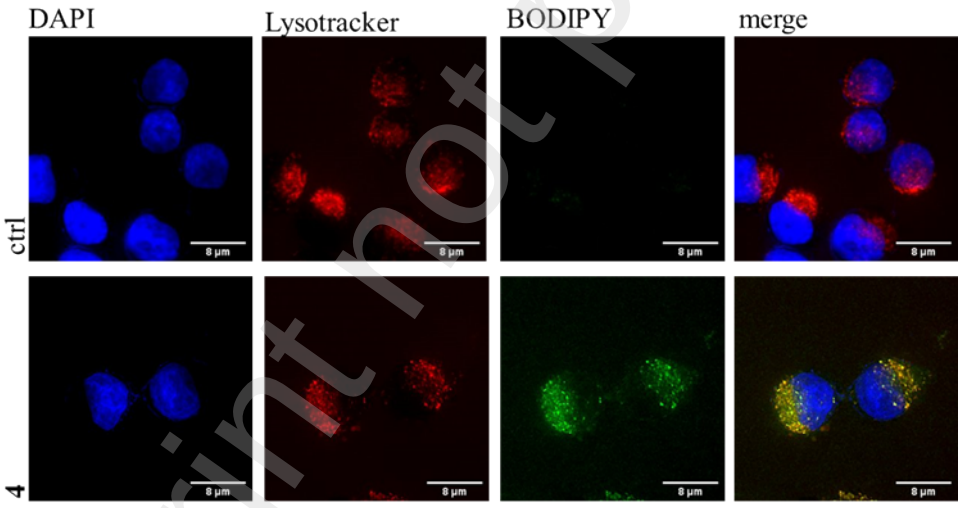

Fig. 2. Fluorescence microscopy images of HeLa cells incubated with BODIPY **4** (1 μM) and Lysotracker RED (0.1 μM). Cells were incubated in serum-free medium with **4** for 1 h and Lysotracker was added to the cells in the last 30 min of incubation. The control was performed according to the same protocol without the addition of **4**. Colocalization can be observed in the "merge" column. Images were taken at 60× magnification under immersion oil. Scale bar = 8 μM.

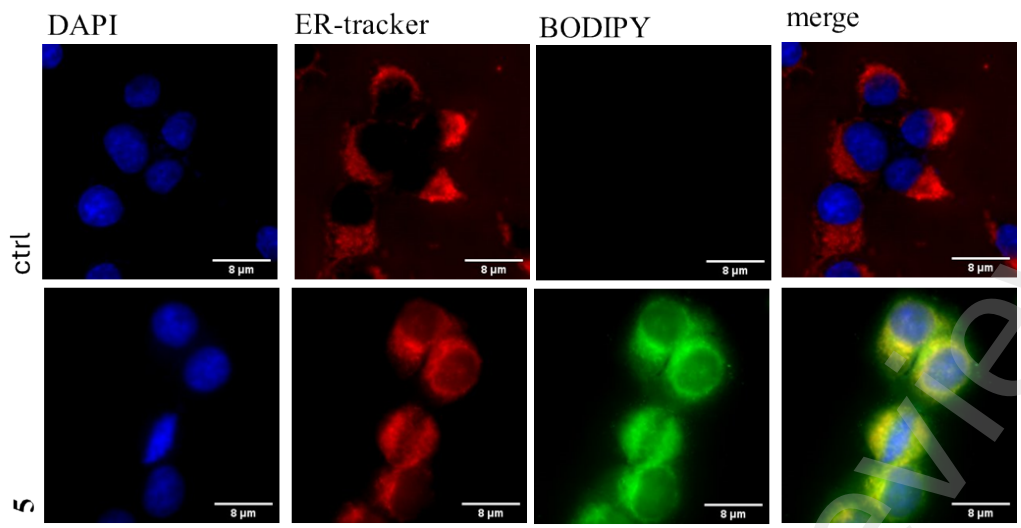

Fig. 3. Fluorescence microscopy images of HeLa cells incubated with BODIPY **5** (5 µM) and ER-tracker red dye (1 µM). Cells were incubated in DMEM with **5** for 30 min and after washing, the ER-tracker was incubated in HBSS for an additional 30 min. The control was performed according to the same protocol without the addition of **5**. Colocalization can be observed in the "merge" column. Images were taken at 60× magnification under immersion oil. Scale bar = 8 µM.

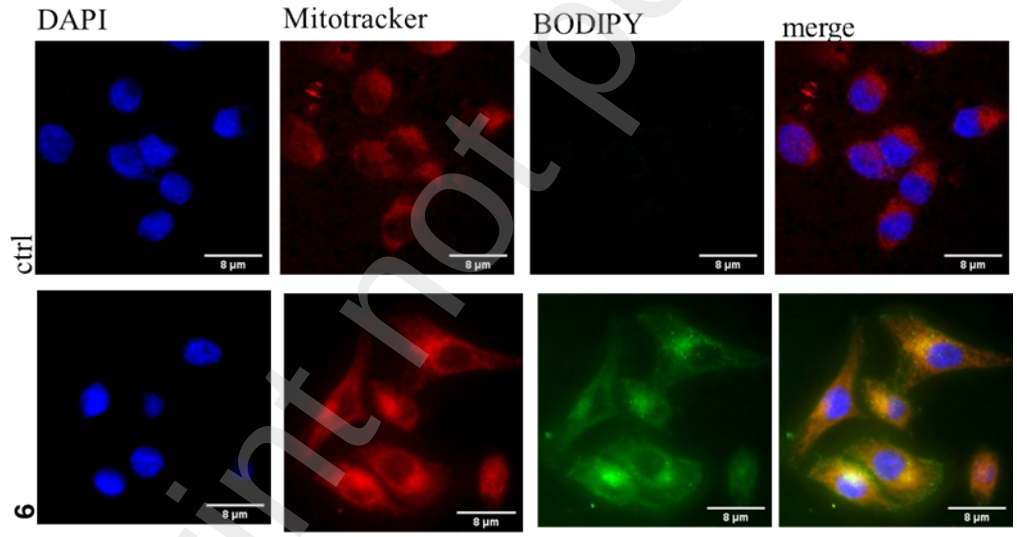

Fig. 4. Fluorescence microscopy images of HeLa cells incubated with BODIPY **6** (5 µM) and Mitotracker RED (0.1 µM). Cells were incubated in DMEM with **6** for 1 h and after washing, the Mitotracker was incubated in HBSS for 30 min. The control was performed according to the same protocol without the addition of **6**. Colocalization can be observed in the "merge" column. Images were taken at 60× magnification under immersion oil. Scale bar = 8 µM.

Conclusion

Here we have demonstrated that the use of simple peptide coupling protocol allows for the synthesis of BODIPY amide derivatives bearing different organelle-targeting groups in the *meso*-position. Furthermore, the use of click-chemistry and the BODIPY alkyne also enables synthetic approach to a variety of BODIPY dyes for selective localization in different intracellular organelles. By use of these protocols, we synthesized BODIPY derivatives **4**-**6**, showed their excellent spectral and photophysical properties and selective localization in lysosomes, endoplasmic reticulum and mitochondria, respectively. Due to selective localization, these dyes show applicability in biology, whereas the synthetic methodologies show potential for the simple and inexpensive preparation of plethora of different organelle-targeting dyes.

Experimental

General

All chemicals and solvents used for the synthesis were analytical or HPLC grade and commercially available. Reactions were monitored using thin layer chromatography (TLC) on silica gel plates (Silica gel 60 F254, Merck, Germany) and by reverse-phase high performance liquid chromatography (RP-HPLC) on a HPLC Agilent 1260Infinity II with DAD detector. The HPLC was performed on an analytical column Phenomenex LC 150 × 4.6 mm, LUNA 3 μm C18(2) 100 Å. For the elution the following method was used: linear gradient from 100% phase B to 100% phase A for 30 min, flow rate 0.8 mL/min, monitored at 254 nm, 366 nm and 500 nm. The solvent system was methanol (A) and 0.1% TFA in methanol/water (1:1; B). The compounds were detected on TLC plates under UV light at 254 nm and 366 nm and on HPLC. The products were purified on silica gel column chromatography on silica gel 60 (0.040–0.063 mm) (Milipore, Germany) and on thin layer preparative liquid chromatography (Silica gel 60 F254, 1 mm and 2 mm, Merck, Germany). Determination and characterization of product structure was carried out by nuclear magnetic resonance (NMR) and high resolution mass spectrometry (HRMS). The NMR spectra were recorded on a Bruker Avance III HD 600 MHz/54 mm Ascend equipped with 5 mm three-channel inversion TCI cryo-probe Prodigy with Z-gradient spiral (model CPP1.1 TCI600S3 H&F-C/N-D-05 Z XT) under the frequency of 600 MHz (^{1}H) and 151 MHz (^{13}C) in $CDCl_3$ or CD_3OD at rt. The spectra were processed in the program MestReNova version 0.2-5475, Mestrelab Research S,L; 2009 and analyzed according to one dimensional (^{1}H and ^{13}C) spectra. Chemical shifts (δ) are expressed according to residual solvent signal. High throughput mass spectrometry analysis was recorded on an UHPLC system Agilent Infinity II 1290. Melting points were determined using a Mikroheiztisch apparatus and were not corrected. Compound names were generated by ChemDraw Professional (version 20.0.0.41) which follows the IUPAC conventions.

4-(5,5-Difluoro-1,3,7,9-tetramethyl-5H-4λ^4,5λ^4-dipyrrolo[1,2-*c*:2',1'-*f*][1,3,2]diazaborinin-10-yl)-*N*-(2-morpholinoethyl)benzamide (4)

Carboxylic acid **7** (50 mg, 0.135 mmol) was dissolved in DMF (1 mL), and then, 4-methyllmorpholine (NMM, 14 mg, 0.148 mmol) and 1-[Bis(dimethylamino)methylene]-1H-

1,2,3-triazolo[4,5-b]pyridine-3-oxide hexafluorophosphate (HATU, 56 mg, 0,148 mmol) were added. The reaction mixture was stirred at rt 15 min, and then, 4-(2-aminoethyl)morpholine (20 mg, 0.148 mmol) was added. The reaction mixture was stirred at rt overnight. DMF was removed on a rotary evaporator and EtOAc (30 mL) and H_2O (30 mL) were added. The extractions with EtOAc (3 × 30 mL) were conducted, the extracts were dried over anhydrous Na_2SO_4, filtered and the solvent was removed on a rotary evaporator. The residue was chromatographed on a silica gel column using CH_2Cl_2/CH_3OH/triethylamine (TEA) 30:2:1 as eluent, to afford pure product **4** (61 mg, 91%) in the form of orange solid.

mp =175-180 °C; ^{1}H NMR (600 MHz, $CDCl_3$,): δ =7.94 (d, *J*=8.3 Hz, 2H), 7.40 (d, *J*=8.3 Hz, 2H), 6.90 (t, *J*=4.1 Hz, 1H), 5.99 (s, 2H), 3.76 (t, *J*= 4.6 Hz, 4H), 3.61 (dd, *J*=5.7 Hz, *J*=11.2 Hz, 2H), 2.65 (t, *J*=6.0 Hz, 2H), 2.57-2.53 (m, 10H), 1.37 (s, 6H); ^{13}C NMR (151 MHz, $CDCl_3$): δ = 166.4, 156.1, 143.0, 140.4, 138.5, 135.0, 131.2, 128.7, 127.9, 121.6, 67.1, 56.9, 53.5, 45.8, 36.3, 14.7, 9.1; HRMS: $C_{26}H_{31}BF_2N_2O_4$ ([M]) found: 480.2617, calculated: 480.2617.

4-(5,5-Difluoro-1,3,7,9-tetramethyl-5H-4λ^4,5λ^4-dipyrrolo[1,2-*c*:2',1'-*f*][1,3,2]diazaborinin-10-il)-*N*-(2-((4-methylphenyl)sulphonamido)ethyl)benzamide (**5**)

Carboxylic acid **7** (91 mg, 0.25 mmol) was dissolved in DMF (1.5 mL), and then, NMM (27 mg, 0.27 mmol) and HATU (107 mg, 0.27 mmol) were added. The reaction mixture was stirred at rt 15 min, and then, over 20 min *N*-(2-aminoethyl)-4-methylbenzensulphonamide (60 mg, 0.27 mmol) was added. The reaction mixture was stirred at rt over 2 days. DMF was removed on a rotary evaporator and EtOAc (20 mL) and H_2O (20 mL) were added. The extractions with EtOAc (3 × 30 mL) were conducted, the extracts were dried over anhydrous $MgSO_4$, filtered and the solvent was removed on a rotary evaporator. The residue was chromatographed on a silica gel column using EtOAc as eluent to afford pure compound **5** (129 mg, 93%) in the form of orange solid.

mp 228-232 °C; ^{1}H NMR (600 MHz, $CDCl_3$): δ = 7.96 (d, *J*=8.3 Hz, 2H), 7.76 (d, *J*=8.3 Hz, 2H), 7.36 (d, *J*= 8.2 Hz, 2H), 7.31 (d, *J*=8.0 Hz, 2H), 7.11 (t, *J*=4.9 Hz, 1H), 5.98 (s, 2H), 5.37 (s, 1H), 3.62 (dd, *J*=5.5 Hz, *J*=10.9 Hz, 2H), 3.22 (dd, *J*=6.1 Hz, *J*=11.0 Hz, 2H), 2.55 (s, 6H), 2.42 (s, 3H), 1.34 (s, 6H); ^{13}C NMR (151 MHz, $CDCl_3$): δ = 167.4, 156.1, 144.1, 143.1, 140.4, 138.7, 136.6, 134.5, 131.2, 130.1, 128.6, 128.1, 127.2, 121.6, 42.9, 40.4, 21.7, 14.7,14.3; HRMS: $C_{29}H_{31}BF_2N_4O_3S$ ([M]) found: 564.2283, calculated: 564.2287.

5,5-difluoro-1,3,7,9-tetramethyl-10-(4-(2-(prop-2-yn-1-yloxy)ethoxy)phenyl)-5H-4λ^4,5λ^4-dipyrrolo[1,2-*c*:2',1'-*f*][1,3,2]diazaborinine (8)

BODIPY phenol **9**[43] (0.29 mmol, 100 mg) was dissolved in acetone (4 mL) at rt. K_2CO_3 (0.87 mmol, 120 mg) and 2-(prop-2-yn-1-yloxy)ethyl 4-methylbenzenesulfonate (0.44, 110 mg) were added, and the reaction mixture was stirred over 24h at 65 °C. The progress of the reaction was monitored by HPLC. The solvent was removed on a rotary evaporator, and to the residue aqueous solution of NH_4Cl (mL) and EtOAc (mL) were added. The extraction with EtOAc were carried out (3×30 mL), the extracts were dried over anhydrous Na_2SO_4, filtered, and the solvent was removed on a rotary evaporator. The residue was purified on a silica gel column using hexane:EtOAc = 4:1 as eluent to afford pure product **8** (97 mg, 78%) in the form of orange oil.

^{1}H NMR (600 MHz, $CDCl_3$): 7.16 (d, *J* = 8.6 Hz, 2H), 7.03 (d, *J* = 8.6 Hz, 2H), 5.97 (s, 2H), 4.30 (d, *J* = 2.4 Hz, 2H), 4.22-4.20 (m, 2H), 3.96-3.94 (m, 2H), 2.55 (br. s, 6H), 2.48 (t, *J* = 2.4

Hz, 1H), 1.42 (br. s, 6H); ^{13}C NMR (151 MHz, $CDCl_3$): 159.4, 155.4, 143.3, 141.9, 131.9, 129.3, 127.5, 121.2, 115.3, 79.4, 75.1, 68.3, 67.4, 58.8, 14.7.

(4-(4-((2-(4-(5,5-difluoro-1,3,7,9-tetramethyl-5H-4l4,5l4-dipyrrolo[1,2-c:2',1'-f][1,3,2]diazaborinin-10-yl)phenoxy)ethoxy)methyl)-1H-1,2,3-triazol-1-yl)butyl)triphenylphosphonium (6) BODIPY-alkyne **8** (0.35 mmol, 150 mg) was dissolved at rt in freshly distilled anhydrous THF (10 mL). CuI (0.07 mmol, 15 mg) and DIPEA (1.49 mmol, 263 μL) were added and the reaction was stirred for 10 min. (4-azidobutyl)triphenylphosphonium bromide **10** (0.69 mmol, 249 mg) was added and the reaction mixture was heated at the temperature of reflux over 24h. The progress of the reaction was monitored by HPLC. The solvent was removed on a rotary evaporator and the residue was purified on thin layer preparative silica gel chromatography using 10% CH_3OH/CH_2Cl_2 as eluent to afford pure product **6** (35 mg, 14%) in the form of orange oil. ^{1}H NMR (600 MHz, $CDCl_3$): 8.17 (s, 1H), 7.83-7.73 (m, 9H), 7.70-7.65 (m, 6H), 7.12 (d, J = 7.6 Hz, 2H), 7.00 (d, J = 7.7 Hz, 2H), 5.95 (br. s, 2H), 4.70 (s, 2H), 4.65 (s, 2H), 4.17 (s, 2H), 3.90 (s, 2H), 3.83 (s, 2H), 2.52 (s, 6H), 2.37 (s, 2H), 1.63 (s, 2H), 1.39 (s, 6H); ^{13}C NMR (151 MHz, $CDCl_3$): 159.4, 155.3, 135.1, 133.9, 133.8 (d, $^3J_{PC}$ = 9.1 Hz), 131.9, 130.7, 130.6 (d, $^2J_{PC}$ = 12.2 Hz), 129.2, 127.2, 124.7, 121.2, 118.5, 117.9, 115.3, 68.8, 67.5, 64.7, 53.6, 48.9, 30.2 (d, $^2J_{PC}$ = 16.6 Hz), 21.9 (d, $^1J_{PC}$ = 51.3 Hz), 19.4, 14.7. HRMS: $C_{46}H_{48}BF_2N_5O_2P$ ([M]) found: 782.3716, calculated: 782.3715.

Investigation of enzymatic stability

Compounds **4** or **5**, were dissolved in 500 μL of 10% DMSO in Tris-SO_4 buffer (pH = 7.0 or pH = 8.8). Enzymes CAL-B or PPL (~ 10 mg) were added, and the reaction mixture was stirred at 37 °C over 24 h. The progress of the reaction was monitored by HPLC, and no changes in the chromatograms were observed.

Photophysical measurements

UV-Vis measurements were performed on a PG T80/T80+ instrument in different solvents. CH_3CN was of spectroscopic grade purity, CH_2Cl_2 was purified by double distillation, and mQ-H_2O from Millipore was used. The fluorescence spectra were measured using an Edinburgh FS5 spectrofluorometer in different solvents at rt (25 °C). For fluorescence measurements absorbance of the solutions at the excitation wavelength was <0.1. Before the measurement, the solutions were purged with N_2 for 20 min. The measurements were performed using slits corresponding to the bandpass of 1.0 nm for the excitation and the emission. The fluorescence quantum yields (Φ_F) were determined using Rhodamine B in methanol (Φ_F = 0.66) as a reference.[42] The relative quantum yields of fluorescence (Φ_F) were obtained by averaging the values calculated from the measurements at different excitation wavelengths (460, 470 and 480 nm) (see Eq. S1 in the SI). Fluorescence decays were measured using TC-SPC on an Edinburgh FS5 spectrofluorometer over 1023 channels. A pulsed laser at 445 nm was used for the excitation and the pulse duration was 20 ps. The time increment per channel was 20 ps. The decays were collected at 510 and 520 nm until they reached 3000 photons in the peak channel. Instrument response function (IRF) was obtained by use of suspension of silica gel in H_2O. Fitting parameters (lifetime, τ, and pre-exponential factors, α) were determined by minimizing the reduced χ^2 value (see Eq. S2 in the SI).

Biological experiments

Cell culture: The cervical adenocarcinoma cell line (HeLa) was cultured in Dulbecco's modified Eagle medium (DMEM) (PanBiotech, Germany) with high glucose content (4.5 g/L), supplemented with 10% fetal bovine serum (FBS) (PanBiotech, Germany) 1% penicillin/streptomycin solution (PanBiotech, Germany) and 1% L-glutamine (Pan Biotech, Germany). Cells were maintained at 37 °C and 5% CO_2 and passaged at 80% confluence by trypsinization with 0.25% trypsin–EDTA (PanBiotech, Germany).

Fluorescence microscopy experiments: Cells were seeded in 12-well plates at a concentration of 50 000 cells/well. A coverslip was placed in each well before the cells were added. The cells were then incubated for 24 h after they had reached full morphology. The cell medium was removed and replaced with a new medium containing BODIPY. Different protocols were used depending on the BODIPY used. For BODIPY **4**, cells were treated with a 1 μM concentration prepared in serum-free medium and incubated for 1 h. After 30 min of incubation, Lysotracker RED DND-99 (ThermoFisher Scientific, USA),[44] prepared in serum-free medium, was added to the BODIPY medium to reach the final concentration of 0.1 μM. After incubation, cells were washed with pre-warmed Dulbecco's phosphate buffer saline (DPBS) (Pan Biotechn, Germany) and fixed with 4% paraformaldehyde for 8 min at rt. With BODIPY **5**, cells were treated with 5 μM solution in DMEM and incubated for 30 min. After the incubation with BODIPY, the cells were washed with HBSS and 1 μM ER-Tracker Red dye (Invitrogen, USA)[45] prepared in HBSS was added to the cells and incubated for 30 min. After the incubation, the cells were washed with pre-warmed DPBS and fixed with 4% paraformaldehyde for 2 min at rt. After the fixation, the cells were washed with PBS. Similar as before, when BODIPY **6** was used, cells were treated with a concentration of 5 μM prepared in DMEM and incubated for 1 h. After the incubation with BODIPY, the cells were washed with Hanks' Balanced Salt Solution (HBSS) without Ca^{2+}, Mg^{2+} (Capricorn Scientific, Germany) and 0.1 μM Mitotracker RED FM (ThermoFisher Scientific, USA),[46] prepared in HBSS, was added to the cells and incubated for 30 min. After the incubation, the cells were washed with pre-warmed DPBS and fixed with 4% paraformaldehyde for 5 min at rt. Subsequently, the cell nuclei in all samples were stained with DAPI (5 mg/mL dissolved in PBS in 1:10000 ratio) and incubated for 3-5 min at rt. DAPI solution was removed, and cells were washed with DPBS and mili-Q water and mounted with Mountain media (Sigma Aldrich, MA, USA) to connect the slips. Images were observed with fluorescence microscopy (Olympus IX83 equipped with Hamamatsu Orca R2 camera) at 60× magnification with immersion oil. BODIPYs were excited in the green (λ = 460-495 nm) wavelength channel, the red (λ = 530-550 nm) channel was used for trackers and the blue (λ = 360-370 nm) channel for DAPI. All images were analyzed with the *ImageJ* program and the Pearson's correlation coefficient were calculated with the JaCoP plugin.

Data Availability Statement: The data underlying this study are available in the published article, in its Supporting Information, and openly available in Public Documents_HrZZ-IP-2019-04-8008 at: https://mojoblak.irb.hr/s/PXPWDXZ2QCp3daC. For microscopy images see the following database: Database (fluorescence microscopy) for a manuscript "BODIPY fluorescent dyes for selective staining of intracellular organelles" | Repozitorij Fakulteta biotehnologije i razvoja lijekova (uniri.hr).

Supporting Information

Supporting information contains detailed experimental procedures for the preparation of all intermediates in the synthesis, UV-vis and fluorescence data, HPLC chromatograms and copies of ^{1}H and ^{13}C NMR spectra. The Supporting Information is available free of charge on the website.

ACKNOWLEDGMENT

This research was funded by Croatian Science Foundation (HRZZ grant no. HRZZ-IP-2019-04-8008). The authors thank Dr. Marijeta Kralj, Dr. Ivo Piantanida and Dr. Dragomira Majhen from the Ruđer Bošković Institute for supplying us with the fluorescent dyes for colocalization experiments. The authors are also grateful for the support from Professor Nela Malatesti for mentoring L.V. and discussion of the results.

REFERENCES

[1] (a) Lichtman, J. W.; Conchello, J.-A. Fluorescence microscopy. *Nature Methods*, **2005**, *2*, 910-919. (b) Combs, C. A. Fluorescence Microscopy: A Concise Guide to Current Imaging Methods. *Curr. Protocols Neurosci.*, Wiley, 2010. (c) Renz, M. Fluorescence Microscopy - Historical and Technical Perspective, *Cytometry Part A*, **2013**, *83A*, 767-779; (d) Hickey, S. M.; Ung, B.; Bader, C.; Brooks, R.; Lazniewska, J.; Johnson, I. R. D.; Sorvina, A.; Logan, J.; Martini, C.; Moore, C. R.; Karageorgos, L.; Sweetman, M. J.; Brooks, D. A. Fluorescence Microscopy-An Outline of Hardware, Biological Handling, and Fluorophore Considerations. *Cells* **2022**, *11*, 35.

[2] (a) Huang, Y.; Cao, X.; Deng, Y.; Ji, X.; Sun, W.; Xia, S.; Wan, S.; Zhang, H.; Xing, R.; Ding, J.; Ren, C. An overview on recent advances of reversible fluorescent probes and their biological applications. *Talanta*, **2024**, *268*, 125275; (b) Kanti Mal, D.; Pal, H.; Chakraborty, G. A comprehensive review on recent advances in fluorescence-based bio-analytes sensing. *TrAC Trends Anal. Chem*., **2024**, *171*, 117493; (c) Khan, J. Synthesis and Applications of Fluorescent Chemosensors: A Review, *J. Fluoresc*, **2023**.(d) Duan, X.; Zhang, M.; Zhang, Y.-H. Organic fluorescent probes for live-cell super-resolution imaging. *Frontiers Optoelectronics*, **2023**, *16*, 34; (e) Wu, D.; Sedgwick, A. C.; Gunnlaugsson, T.; Akkaya, E. U.; Yoon, J.; James, T. D. Fluorescent chemosensors: the past, present and future. *Chem. Soc. Rev*., **2017**, *46*, 7105-7123.

[3] Haugland, R. P. The Handbook. A Guide to Fluorescent Probes and Labeling Technologies, 10th ed.; Molecular Probes, Inc.: Eugene, Oregon, USA, 2005.

[4] Zhu, H.; Fan, J.; Du, J.; Peng, X. Fluorescent Probes for Sensing and Imaging within Specific Cellular Organelles. *Acc. Chem. Res*. **2016** 49, 2115-2126.

[5] Treibs, A.; Kreuzer, F.-H. Difluorboryl-Komplexe von Di- und Tripyrrylmethenen. *Liebigs Ann. Chem*. **1968**, 718, 208-223.

[6] Loudet, A.; Burgess, K. BODIPY Dyes and Their Derivatives: Syntheses and Spectroscopic Properties. *Chem. Rev*. **2007**, 107, 4891-4932.

[7] Ulrich, G.; Ziessel, R.; Harriman, A. The chemistry of fluorescent BODIPY dyes: versatility unsurpassed. *Angew. Chem. Int. Ed*. **2008**, *47*, 1184-1201.

[9] Bumagina, N. A.; Antina, E. V.; Ksenofontov, A. A.; Antina, L. A.; Kalyagin, A. A.; Berezin, M. B. Basic structural modifications for improving the practical properties of BODIPY. *Coord. Chem. Rev*. **2022**, *469*, 214684.

[10] Yadav, I. S.; Misra, R. Design, synthesis and functionalization of BODIPY dyes: applications in dye-sensitized solar cells (DSSCs) and photodynamic therapy (PDT). *J. Mater. Chem. C* **2023**, *11*, 8688-8723.

[11] Boens, N., Leen, V.; Dehaen, W. Fluorescent indicators based on BODIPY. *Chem. Soc. Rev.* **2012**, *41*, 1130–1172.

[12] (a) Awuah, S. G.; You, Y. Boron dipyrromethene (BODIPY)-based photosensitizers for photodynamic therapy. *RSC Advances* **2012**, *2*, 11169-11183. (b) Kamkaew, A.; Lim, S. H.; Lee, H. B.; Kiew, L. V.; Chug, L. Y.;Burgess, K. BODIPY dyes in photodynamic therapy. *Chem. Soc. Rev.* **2013**, *42*, 77-88. (c) Turksoy, A.; Yildiz, D.; Akkaya, E. U. Photosensitization and controlled photosensitization with BODIPY dyes. *Coord. Chem. Rev.* **2019**, *379*, 47-64. (d) Prieto-Montero, R.; Prieto-Castañeda, A.; Sola-Llano, R.; Agarrabeitia, A. R.; García-Fresnadillo, D.; López-Arbeloa, I.; Villanueva, A.; Ortiz, M. J.; de la Moya, S.; Martínez-Martínez, V. Exploring BODIPY Derivatives as Singlet Oxygen Photosensitizers for PDT. *Photochem. Photobiol.* **2020**, *96*, 458-477. (e) Malacarne, M. C.; Gariboldi, M. B. BODIPYs in PDT: A Journey through the Most Interesting Molecules Produced in the Last 10 Years. *Int. J. Mol. Sci.* **2022**, *23*, 10198. (f) Zhang, W.; Ahmed, A.; Cong, H.; Wang, S.; Shen, Y.; Yu, B. Application of multifunctional BODIPY in photodynamic therapy. *Dyes and Pigments* **2021**, *185*, 108937.

[13] (a) Kowada, T.; Maeda, H.; Kikuchi, K. BODIPY-based probes for the fluorescence imaging of biomolecules in living cells. *Chem. Soc. Rev.* **2015**, *44*, 4953-4972. (b) Xu, W.; Zeng, Z.; Jiang, J. – H.; Chang, Y. – T.; Yuan, L. Discerning the Chemistry in Individual Organelles with Small-Molecule Fluorescent Probes. *Angew. Chem. Int. Ed.* **2016**, *55*, 13658-13699. (c) Wang, S.; Gao, X.; Zhang, X.; Huan, S.; Wang, L.; Li, J.; Zhang, G.; Zhang, X. Targeted BODIPY dyes for small molecule recognition. *Chem. Soc. Rev.* **2024**, *53*, 3974.

[8] Boens, N.; Verbelen, B.; Ortiz, M. J.; Jiao, L.; Dehaen, W. Synthesis of BODIPY dyes through postfunctionalization of the boron dipyrromethene core. *Coord. Chem. Rev.* **2019**, *399*, 213024.

[14] Shrestha, P.; Kand, D.; Weinstain, R.; Winter, A. H. *meso*-Methyl BODIPY Photocages: Mechanisms, Photochemical Properties, and Applications. *J. Am. Chem. Soc*. **2023**, *145*, 32, 17497-17514.

[15] Singh, P. K.; Majumdar, P.; Singh, S. P. Advances in BODIPY photocleavable protecting groups. *Coord Chem Rev*. **2021**, *449*, 214193.

[16] Toupin, N. P.; Arora, K.; Shrestha, P.; Peterson, J. A.; Fischer, L. J.; Rajagurubandara, E.; Podgorski, I.; Winter, A. H.; Kodanko, J. J. BODIPY-Caged Photoactivated Inhibitors of Cathepsin B Flip the Light Switch on Cancer Cell Apoptosis. *ACS Chem. Biol*. **2019**, *14*, 2833-2840.

[17] Sitkowska, K.; Hoes, M. F.; Lerch, M. M.; Lameijer, L. N.; Van Der Meer, P.; Szymański, W.; Feringa, B. L. Red-light-sensitive BODIPY photoprotecting groups for amines and their biological application in controlling heart rhythm. *Chem. Commun*. **2020**, *56*, 5480-5483.

[18] Wijesooriya, C. S.; Peterson, J. A.; Shrestha, P.; Gehrmann, E. J.; Winter, A. H.; Smith, E. A. A Photoactivatable BODIPY Probe for Localization-Based Super-Resolution Cellular Imaging. *Angew. Chem. Int. Ed*. **2018**, *57*, 12685-12689.

[19] Kand, D.; Pizarro, L.; Angel, I.; Avni, A.; Friedmann-Morvinski, D.; Weinstain, R. Organelle-Targeted BODIPY Photocages: Visible-Light-Mediated Subcellular Photorelease. *Angew. Chem. Int. Ed*. **2019**, *58*, 4659-4663.

[20] Kand, D.; Liu, P.; Navarro, M. X.; Fischer, L. J.; Rousso-Noori, L.; Friedmann-Morvinski, D.; Winter, A. H.; Miller, E. W.; Weinstain, R. Water-Soluble BODIPY Photocages with Tunable Cellular Localization. *J. Am. Chem. Soc.* **2020**, *142*, 4970-4974.

[21] Poryvai, A.; Galkin, M.; Shvadchak, V.; Slanina, T. Red-Shifted Water-Soluble BODIPY Photocages for Visualisation and Controllable Cellular Delivery of Signaling Lipids. *Angew. Chem. Int. Ed*. **2022**, *61*, e202205855.

[22] (a) Yang, J.; Zhang, R.; Zhao, Y.; Tian, J.; Wang, S.; Gros, C. P.; Xu, H. Red/NIR neutral BODIPY-based fluorescent probes for lighting up mitochondria. Red/NIR neutral BODIPY-based fluorescent probes for lighting up mitochondria. *Spectrochim. Acta A. Mol Biomol. Spect.* **2021**, *248*, 119199. (b) Zhang, X.; Xiao, Y.; Qi, J.; Qu, J.; Kim, B.; Yue, X. Belfield, K. D. Long-wavelength, photostable, two-photon excitable BODIPY fluorophores readily modifiable for molecular probes. *J. Org. Chem*. **2013**, *78*, 9153-9160; (c) Sui, B.; Tang, S.; Woodward, A. W.; Kim, B.; Belfield, K. D. A BODIPY-Based Water-Soluble Fluorescent Probe for Mitochondria Targeting. *Eur. J. Org. Chem*. 2016, 2851-2857. (d) Jiang, N.; Fan, J.; Liu, T.; Cao, J.; Qiao, B.; Wang, J.; Gao, P.; Peng, X. A near-infrared dye based on BODIPY for tracking morphology changes in mitochondria. *Chem. Commun*. **2013**, *49*, 10620-10622. (e) Zhang, S.; Wu, T.; Fan, J.; Li, Z.; Jiang, N.; Wang, J.; Dou, B.; Sun, S.; Song, F.; Peng, X. A BODIPY-based fluorescent dye for mitochondria in living cells, with low cytotoxicity and high photostability. *Org. Biomol. Chem*. **2012**, *11*, 555-558.

[23] (a) Zhang, Y. Z.; Diwu, Z. P.; Haugland, R., US5869689A, 1999. (b) Freundt, E. C.; Czapiga, M.; Lenardo, M. J. Photoconversion of Lysotracker Red to a green fluorescent molecule. *Cell Res*. **2007**, *17*, 956-598. (c) Kong, X.; Di, L.; Fan, Y.; Zhou, Z.; Feng, X., Gai, L.; Tian, J.; Lu, H. Lysosome-targeting turn-on red/NIR BODIPY probes for imaging hypoxic cells. *Chem. Commun.*, **2019**, *55*, 11567-11570. (d) Ye, Z.; Xiong, C.; Pan, J.; Su, D.; Zeng, L. Highly photostable, lysosome-targeted BODIPYs with green to near-infrared emission for lysosome imaging in living cells. *Dyes and Pigments*. **2018**, *155*, 30-35. (e) Gonçalves, R. C. R.; Belmonte-Reche, E.; Pina, J.; Costa da Silva, M.; Pinto, S. C. S.; Gallo, J.; Costa, S. P. G.; Raposo, M. M. M. Bioimaging of Lysosomes with a BODIPY pH-Dependent Fluorescent Probe. *Molecules*, **2022**, *27*, 8065.

[24] (a) Bousseksou, A.; Salmon, L.; Cobo, S., WO2011058277A1. 2011. (b) de Jong, F.; Pokorny, J.; Manshian, B.; Daelemans, B.; Vandaele, J.; Startek, J. B.; Soenen, S.; Van der Auweraer, M.; Dehaen, W.; Rocha, S.; Silveira-Dorta, G. Development and characterization of BODIPY-derived tracers for fluorescent labeling of the endoplasmic reticulum. *Dyes and Pigments* **2020**, *176*, 108200. (c) Lee, H.; Yang, Z.; Wi, Y.; Kim, T. W.; Verwilst, P.; Lee, Y. H.; Han, G.-I.; Kang, C.; Kim, J. S. BODIPY-Coumarin Conjugate as an Endoplasmic Reticulum Membrane Fluidity Sensor and Its Application to ER Stress Models. *Bioconjug. Chem*. **2015**, *26*, 2474-2480. (d) Xu, W.; Zeng, Z.; Jiang, J. H.; Chang, Y. T.; Yuan, L. Wahrnehmung der chemischen Prozesse in einzelnen Organellen mit niedermolekularen Fluoreszenzsonden. *Angew. Chem*. **2016**, *128*, 13858-13902. (e) Yang, Z.; Wi, Y.; Yoon, Y. M.; Verwilst, P.; Jang, J. H.; Kim, T. W.; Kang, C.; Kim, J. S. BODIPY/Nile-Red-Based Efficient FRET Pair: Selective Assay of Endoplasmic Reticulum Membrane Fluidity. *Chem. Asian J*. **2016**, *11*, 527-531. (f) Yang, Z.; He, Y.; Lee, J.H.; Chae, W. S.; Ren, W. X.; Lee, J. H. Kang, C.; Kim, J. S. A Nile Red/BODIPY-based bimodal probe sensitive to changes in the micropolarity and microviscosity of the endoplasmic reticulum. *Chem. Commun*. **2014**, *50*, 11672-11675.

[25] Pagano, R. E.; Martin, O. C.; Kang, H. C.; Haugland, R. P. A novel fluorescent ceramide analogue for studying membrane traffic in animal cells: accumulation at the Golgi apparatus results in altered spectral properties of the sphingolipid precursor. *J. Cell. Biol*. **1991**, *113*, 1267-1279.

[26] Nakamura, A.; Takigawa, K.; Kurishita, Y.; Kuwata, K.; Ishida, M.; Shimoda, Y.; Hamachi, I.; Tsukiji, S. Hoechst tagging: a modular strategy to design synthetic fluorescent probes for live-cell nucleus imaging. *Chem. Commun*. **2014**, *50*, 6149-6152.
[27] Zhang, Y.; Fang, H.-M.; Zhang, X.-T.; Wang, S.; Xing, G.-W. 8-(4-aminophenyl)-BODIPYs as fluorescent pH probes: facile synthesis, computational study and lysosome imaging. *Chem. Select* **2016**, 1, 1-6.
[28] Gao, T.; He, H.; Huang, R.; Zheng, M.; Wang, F.-F.; Hu, Y.-J.; Jiang, F.-L.; Liu, Y. BODIPY-based fluorescent probes for mitochondria-targeted cell imaging with superior brightness, low cytotoxicity and high photostability. *Dyes and Pigments*, **2017**, *141*, 530-535.
[29] Murphy, M. P.; Hartley, R. C. Mitochondria as a therapeutic target for common pathologies. *Nature Rev*. **2018**, *17*, 865-885.
[30] Schwarz, D. S.; Blower, M. D. The endoplasmic reticulum: structure, function and response to cellular signalling. *Cell. Mol. Life Sci*. **2016**, *73*, 79-94.
[31] Trybus, W.; Trybus, E.; Król, T. Lysosomes as a Target of Anticancer Therapy. *Int. J. Mol. Sci.* **2023**, *24*, 2176.
[32] Sakhrani, N. M.; Padh, H. Organelle targeting: third level of drug targeting. *Drug Des. Devel. Ther*. **2013**, *7*, 585-599.
[33] HATU = 1-[Bis(dimethylamino)methylene]-1*H*-1,2,3-triazolo[4,5-*b*]pyridinium 3-oxide hexafluorophosphate; (a) Carpino, L. A.; 1-Hydroxy-7-azabenzotriazole. An Efficient Peptide Coupling Additive. *J. Am. Chem. Soc*., **1993**, *115*, 4397-4398. (b) Carpino, L.A.; Imazumi, H.; El-Faham, A.; Ferrer, F. J.; Zhang, C.; Lee, Y.; Foxman, B. M.; Henklein, P.; Hanay, C.; Mügge, C.; Wenschuh, H.; Klose, J.; Beyermann, M.; Bienert, M. The uronium/guanidinium peptide CouplingReagents: finally the true uronium salts. *Angew. Chem. Int. Ed*. **2002**, *41*, 441-445.
[34] Kolb, H. C.; Finn, M. G.; Sharpless, K. B. Click Chemistry: Diverse Chemical Function from a Few Good Reactions. *Angew. Chem. Int. Ed*. **2001**, *40*, 2004-2021.
[35] (a) Kazlauskas, R. J. Enhancing catalytic promiscuity for biocatalysis. *Curr. Opinion Chem. Biol*. **2005**, *9*, 195-201. (b) van Rantwijk, F.; Sheldon, R. A. Enantioselective acylation of chiral amines catalysed by serine hydrolases. *Tetrahedron* **2004**, *60*, 501-519.
[36] (a) Mendes, A. A.; Oliveira, P. C.; de Castro, H. F. Properties and biotechnological applications of porcine pancreatic lipase. *J. Mol. Catal. B: Enzymatic*, **2012**, *78*, 119-134; (b) Hertweck, C.; Boland, W. Porcine pancreatic lipase (PPL) - a versatile biocatalyst in organic synthesis. *J. Prakt. Chem*. **1997**, *339*, 200-202.
[37] Qin, W.; Baruah, M.; Van der Auweraer, M.; De Schryver, F. C.; Boens, N. Photophysical Properties of Borondipyrromethene Analogues in Solution. *J. Phys. Chem. A* **2005**, *109*, 7371-7384.
[38] Tian, M.; Peng, X.; Feng, F.; Meng, S.; Fan, J.; Sun, S. Fluorescent pH probes based on boron dipyrromethene dyes. *Dyes and Pigments* **2009**, *81*, 58-62.
[39] (a) Kollmannsberger, M.; Rurack, K.; Resch-Genger, U.; Daub, J. Ultrafast Charge Transfer in Amino-Substituted Boron Dipyrromethene Dyes and Its Inhibition by Cation Complexation: A New Design Concept for Highly Sensitive Fluorescent Probes. *J. Phys. Chem. A* **1998**, *102*, 10211-10220. (b) Werner, T.; Huber, C.; Heinl, S.; Kollmannsberger, M.; Daub, J.; Wolfbeis, O. S. Novel optical pH-sensor based on a boradiaza-indacene derivative. *Fresenius J. Anal Chem*. **1997**, *359*, 150-154. (c) Rurack, K.; Kollmannsberger, M.; Daub, J. A highly efficient sensor molecule emitting in the near infrared (NIR): 3,5-distyryl-8-(p-dimethylaminophenyl)difluoroboradiaza-s-indacene. *New. J. Chem*. **2001**, *25*, 289-292.
[40] (a) Esnal, I.; Bañuelos, J.; López Arbeloa, I.; Costela, A.; Garcia-Moreno, I.; Garzón, M.; Agarrabeitia, A. R.; José Ortiz, M. Nitro and amino BODIPYS: crucial substituents to modulate their photonic behavior. *RSC Advances*, **2013**, *3*,1547-1556. (b) Wang, S.; Liu, H.; Mack, J.;

Tian, J.; Zou, B.; Lu, H.; Li, Z.; Jiang, J.; Shen, Z. A BODIPY-based 'turn-on' fluorescent probe for hypoxic cell imaging. *Chem. Commun*. **2015**, *51*, 13389-13392. (c) Gil de Melo, S. M.; Dias de Rezende, L. C.; Petrilli, R.; Vianna Lopez, R. F.; Goulart, M. O. F.; da Silva Emery, F. Nitrosation of BODIPY dyes and their applications in the development of thiol sensors. *Dyes and Pigments* **2020**, *173*, 107885. (d) Mohammed Ali, A.; Wang, W.; Chen, Q.-Y. Structure and biomolecular recognition of nitro-BODIPY-andrographolide assembles for cancer treatment. *Spectrochim. Acta A: Mol. Biomol. Spect*. **2021**, *263*, 120180. (e) Glavaš, M.; Zlatić, K.; Jadreško, D.; Ljubić, I.; Basarić, N. Fluorescent pH sensors based on BODIPY structure sensitive in acidic media. *Dyes and Pigments* **2023**, *220*, 111660

[41] (a) Qin, W.; Rohand, T.; Baruah, M.; Stefan, A.; Van der Auweraer, M.; Dehaen, W.; Boens, N. Solvent-dependent photophysical properties of borondipyrromethene dyes in solution. *Chem. Phys. Lett*. **2006**, *420*, 562-568. (b) Rohand, T.; Lycoops, J.; Smout, S.; Braeken, E.; Sliwa, M.; Van der Auweraer, M.; Dehaen, W.; De Borggraeve W. M.; Boens, N. Photophysics of 3,5-diphenoxy substituted BODIPY dyes in solution. *Photochem. Photobiol. Sci*. **2007**, *6*, 1061-1066. (c) Cieślik-Boczula, K.; Burgess, K.; Li, L.; Nguyen, B.; Pandey, L.; De Borggraeve, W. M.; Van der Auweraer, M.; Boens, N. Photophysics and stability of cyanosubstituted boradiazaindacene dyes. *Photochem. Photobiol. Sci*. **2009**, *8*, 1006-1015.

[42] Boens, N.; Qin, W.; Basarić, N.; Hofkens, J.; Ameloot, M.; Pouget, J.; Lefèvre, J.-P.; Valeur, B.; Gratton, E.; van de Ven, M.; Silva, Jr., N. D.; Engelborghs, Y.; Willaert, K.; Sillen, A.; Rumbles, G.; Phillips, D.; Visser, A. J. W. G.; van Hoek, A.; Lakowicz, J. R.; Malak, H.; Gryczynski, I.; Szabo, A. G.; Krajcarski, D. T.; Tamai, N.; Miura, A. Fluorescence Lifetime Standards for Time and Frequency Domain Fluorescence Spectroscopy. *Anal. Chem.* **2007**, *79*, 2137-2149.

[43] Zlatić, K.; Antol, I.; Uzelac, L.; Mikecin Dražić, A.-M.; Kralj, M.; Bohne, N.; Basarić, N. Labeling of Proteins by BODIPY-Quinone Methides Utilizing Anti-Kasha Photochemistry. *ACS Appl. Mater. Interfaces* **2020**, *12*, 347-351.

[44] Lysotracker RED DND-99 = 3-[2,2-difluoro-12-(1*H*-pyrrol-2-yl)-3-aza-1-azonia-2-boranuidatricyclo[7.3.0.0^{3,7}]dodeca-1(12),4,6,8,10-pentaen-4-yl]-*N*-[2-(dimethylamino)ethyl]propanamide

[45] ER-Tracker Red = 1-((5-chloro-3-(((4-((((cyclohexyl-l2-azaneyl)carbonyl)-l2-azaneyl)sulfonyl)phenethyl)-l2-azaneyl)carbonyl)-2-methoxyphenyl)-l2-azaneyl)-2-(4-(5,5-difluoro-7-(thiophen-2-yl)-5H-4l4,5l4-dipyrrolo[1,2-c:2',1'-f][1,3,2]diazaborinin-3-yl)phenoxy)ethan-1-one

[46] Mitotracker RED FM = (2*Z*)-1-[[4-(chloromethyl)phenyl]methyl]-3,3-dimethyl-2-[(2*E*,4*E*)-5-(1,3,3-trimethylindol-1-ium-2-yl)penta-2,4-dienylidene]indole chloride